Model for Loss Calculation of Wireless In-Wheel Motor Concept Based on Magnetic Resonant Coupling

Motoki Sato
Department of Advanced Energy,
The University of Tokyo, 5-1-5, Kashiwa no ha, Kashiwa city,
Chiba 277-8561, Japan TEL:+814-7136-3881,
(e-mail: satoum@hflab.k.u-tokyo.ac.jp)
Engineering Research Division, Toyodenki Seizo K.K.
3-8, Fukuura, Kanazawa-ku,
YOKOHAMA, Japan 236-000
Tel:+814-5785-3702
(e-mail: satoum@toyodenki.co.jp)

Giuseppe Guidi
Electric Power System Department, Sintef Energy,
PO Box 4761 Sluppen,
No-7465 Trondheim Sem Sæland vei 11,
Trondheim,Norway,
TEL: +47-73-59-7183,
(e-mail:giuseppe.guidi@sintef.no)

Takehiro Imura
Power Frontier Endowed Chair,
Department of Electrical Engineering &
Information Systems Center for Advanced Power &
Environmental Technology School of Engineering. 7-3-1,
Hongo, Bunkyo-ku, Tokyo 113-8656, Japan.
Tel:+81-3-5841-6392,
(e-mail:imura@hori.k.u-tokyo.ac.jp).

Hiroshi Fujimoto
Department of Advanced Energy,
The University of Tokyo,
5-1-5, Kashiwa no ha, Kashiwa city,
Chiba 277-8561, Japan,
(e-mail: fujimoto@k.u-tokyo.ac.jp).

***Abstract*—Adopting the In-Wheel Motor technology (IWM) for the traction system of electric vehicles (EVs) leads to several advantages. Since the motors can drive each wheel in the vehicle independently, the EV can take full advantages of technologies such as anti-slip control of tires for enhanced safety and performance, and optimal torque distribution for extension of the vehicle mileage. However, a major problem of conventional IWM is that the power cables and signal wires from the vehicle body to the wheel are exposed to harsh environment, and may be damaged due to continuous bending, impact with debris from the road, or become brittle because of the freezing in snowy areas. To overcome this problem, a system in which the IWM receives its power wirelessly from the vehicle body has been proposed, resulting in the Wireless In-Wheel Motor (W-IWM) concept. This cutting-edge technology eliminates the risk of cable disconnection of IWM and therefore raises the reliability of the whole vehicle system. Due to steering and to the operation of suspensions, the relative position between the car body and the wheel assembly changes during driving. Therefore, the wireless power transfer has been implemented using the principle of magnetic resonant coupling, which is robust to misalignment between the transmitter and receiver coils. A single phase inverter is installed in the car body side (transmitter side). Single phase converter is also installed the wheel side (receiver side). This paper discusses two control schemes on transmitter side and three control schemes on receiver side. The loss analysis of each converter aims to verify the most efficient control combination. Eventually, the DC/DC chopper control regulating the inverter output voltage amplitude is selected because of its better efficiency compared to other control schemes on transmitter side. In addition, this paper proposes symmetric synchronous rectification control on receiver side. The proposed control effectiveness is confirmed by numerical analysis considering its efficiency and total harmonic distortion.**

***Keywords*—Wireless power transfer, Electric vehicle, Magnetic resonant coupling.**

I. Introduction

In recent years, global environmental issues have been increasing. Although the conventional automobile is convenient. However, it emits polluting gas and mentioned that gasoline resources are limited. Therefore, low emission vehicles are necessary. Among them, electric vehicles (EVs) are a notable alternative. In fact, EVs' torque response is two orders faster compared to the one of an internal combustion engine vehicle. This is an excellent control performance. In particular, various papers about EVs with in-wheel motor for each of the four driving wheels have been studied from that perspective.

- Since the differential gear and drive shaft are unnecessary, the car design has less constraints. Moreover, it is also possible to reduce the weight of the whole car body; according to, the whole drive system will be 36% lighter. Therefore, energy losses are reduced[4].
- Motion controllability and vehicle stability are improved because of each wheel can be controlled independently.

978-1-5090-1815-4/16/$31.00

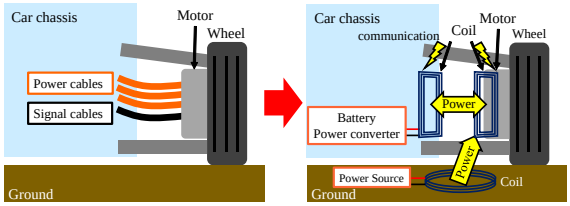

Conventional IWM

Wireless IWM
(W-IWM)

Fig. 1. The concept of W-IWM.

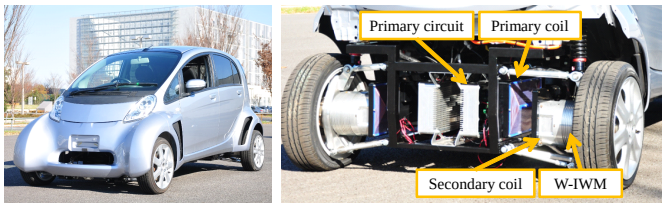

(a) FPEV4-$Sawyer$ (b) First trial unit

Fig. 2. Test vehicle and prototype unit.

TABLE I
TARGET VALUE OF THE VEHICLE PERFORMANCE AND THE FIRST PROTOTYPE GOAL.

	Final target	First target
Number of in-wheel motor	4	2
Rated output power	48 kW	6.6 kW
Rated wheel torque	1300 Nm	475 Nm
Dynamic charging from road	possible	N/A

Currently, the in-wheel motor system has the following issues.

- The driving comfort deteriorates because the unsprung weight is increased.
- The power and signal cables might be disconnected from prolonged and repetitive bending as well as small debris impact or freeze in cold regions.

The first problem can be solved by using the anti-dive force control of the in-wheel motor[4]. The second problem has been tackled by increasing durability and reliability of the cables[5]. However, this is still not sufficient to guarantee the safe transmission of input signal and electric power. Therefore, a novel solution consisting in a bidirectional power transmission system between car body and a wheel has been proposed. A prototype has been built and test runs have been conducted. This structure is called Wireless In-Wheel Motor (W-IWM). In this circuit, coils for wireless power transfer and communication system are installed in the wheel and the car body, thus eliminating the cables in between. The relative position of the power transmitting and receiving coil changes with the movement of the suspension in the actual car body. Consequently, the authors' choice is the magnetic resonant coupling for wireless power transfer[6], [7]. Since the W-IWM is capable of both receiving and transmitting power, it also allows for regenerating energy when the vehicle is decelerating. With this technology, dynamic charging where electric vehicles are powered by devices embedded is the highway surface are a definite possibility in future. It is well known that the receiver side coil voltage and current fluctuate because of the variation of either the coils relative position or the load[8]. Furthermore, in the case of a constant power load, the secondary side load voltage is unstable[9]. Therefore, controlling the voltage or the current by converters in both transmitter and receiver side is necessary for the stable operation of the W-IWM[10].

This paper is organized as follows: in Section II a brief introduction of WIWM and wireless power transfer is provided. In Section III the concept of high efficiency by primary side is explored via loss model while in Section IV the same reasoning is applied to the secondary side. In Section V the system loss breakdown as well as the simulation and experimental results are presented. Finally, in Section VI there is the summary of this paper.

II. WIRELESS IN-WHEEL MOTOR.

A. Expected vehicle performance.

The in-wheel motor conceptual scheme is shown in 1. The vehicle for the experiment, FPEV4-$Sawyer$, shown in 2(a), has been developed in the authors' laboratory at the University of Tokyo[11].

This vehicle has a replaceable sub-unit configuration for both the front and rear wheels, consequently it can test and compare a wide variety of drive units on the same platform. The sub-unit in the prototype is shown in 2(b). In Table I, the vehicle specifications are reported. The final target output power is 48 kW with all the wheel, while the first trial output power is 6.6 kW by using the two rear wheels. In other words, the aim is a continuous rated output power of 3.3 kW per wheel, a necessary parameter for designing a large power transmission control and the coils. In addition, considering the space between the in-wheel motor and the body necessary to the suspension stroke, the gap between the transmitting and receiving coils is set to 100 mm.

B. Wireless power transmission of the magnetic resonant coupling method

In the wireless power transmission by magnetic resonant coupling method adopted in the W-IWM, matching the resonant frequency of the LC circuit used in the coils is mandatory. The operation point angular frequency of the primary-side inverter is

$$\omega_0 = \frac{1}{\sqrt{L_1 C_1}} = \frac{1}{\sqrt{L_2 C_2}}, \quad (1)$$

where L_1 and L_2 as primary and secondary coil inductance, respectively; similarly, C_1 and C_2 are the primary and secondary coil resonant capacitors. In this paper the coils and their relative resonant capacitors form the system, referred to as resonator. Furthermore, the vehicle body side becomes the primary side (power transmission side) and the in-wheel

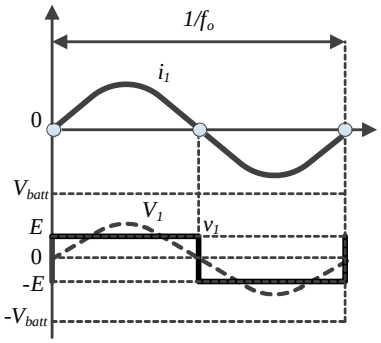

Fig. 4. chopper mode concept

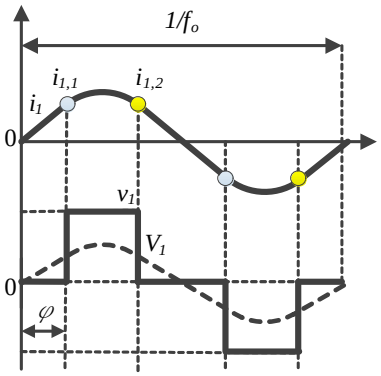

Fig. 5. phase shift mode concept

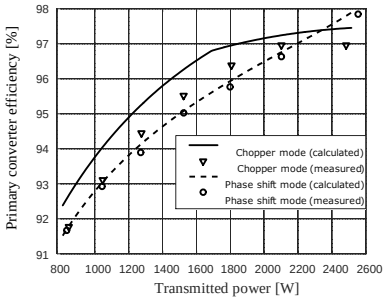

Fig. 6. experimental results and the calculated result of primary converter efficiency

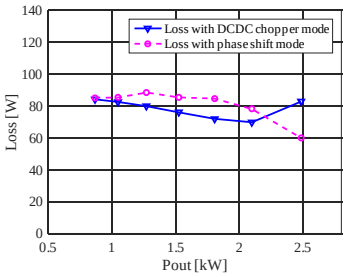

Fig. 7. Primary converter loss of chopper mode vs phase shift mode

motor is considered the secondary side (power receiving side). Finally, the resonant frequency $f_0(=\omega_0/2\pi)$, is assumed to be 85 kHz, in compliance to the international standards for static wireless power transmission to electric vehicles[12].

III. High efficiency of the W-IWM system in primary side

This section introduces the high efficiency control of W-IWM converter. Fig. 3 shows a circuit configuration diagram of a W-IWM. In order to use the same configuration of the actual WIWM, the resonant frequency is considered to be 85 kHz. The output power of the power transmission circuit in (the input power of the resonator) P can be expressed as follows[13].

$$P = \frac{V_1 V_2}{2\pi f_0 L_m} \tag{2}$$

The output voltage fundamental wave RMS value of the transmission-side inverter V_1 must be generated from the vehicle battery voltage V_{batt}. Here, a two-stage power conversion system is adopted. Then, a variable DC-link voltage E is generated as DC/DC converter output voltage and used as a DC-link voltage of the subsequent single-phase H bridge inverter. In the AC side, the voltage is operated as a variable amplitude square wave. This is called chopper mode. The power receiving side (wheel side) is equipped with single-phase H bridge converter and generates an inverter DC-link voltage V_{dc} used to drive the IWM. Receiving-side output AC voltage of the resonator is defined as V_2.

Another method used for generating a variable AC voltage V_1 from another V_{batt} is phase shift method. In this method, by controlling the pulse width, it is possible to control the power sent from the primary side. In this case, the DC/DC converter is bypassed and therefore no losses are generated.

The basic operation of these two power conversion systems is shown in Fig. 4 and Fig. 5. In chopper mode, the switching loss of the H-bridge inverter is minimized; on the other hand the DC/DC converter switching pattern for manipulating E results in increased switching losses as well as conduction losses and core losses of the inductor.

Loss model of the phase shift method is described as follows. Fig. 5 shows the phase shift of the H-bridge inverter output voltage $V_{1,phsh}$. $V_{1,phsh}$ can be expressed as follows.

$$V_{1,phsh} = \frac{2\sqrt{2}}{\pi} V_{batt} \cdot \cos\varphi \tag{3}$$

Where, φ is the phase of zero voltage. If the system is operated at resonance frequency, the resonator current is the fundamental wave component in phase with the quasi sine wave voltage. As a result, the switching currents $I_{1,1}$ and $I_{1,2}$ are calculated as follows.

$$\begin{aligned} I_{1,1} = I_{1,2} &= I_{1,pk}\sin\varphi \approx \sqrt{2}\frac{\mathrm{P}}{\mathrm{V_1}}\sin\varphi \\ &= \frac{\sqrt{2}V_2}{2\pi f_0 L_m}\sin\varphi \end{aligned} \tag{4}$$

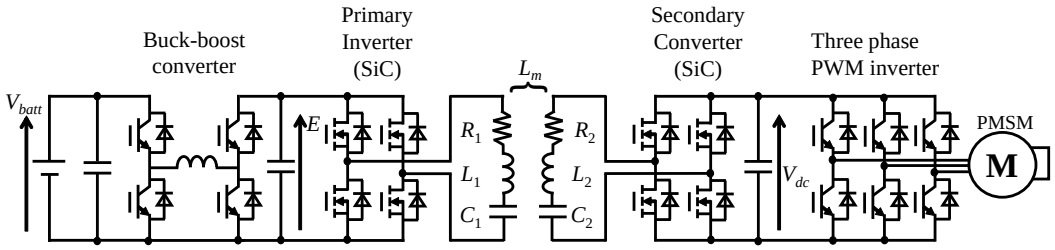

Fig. 3. wireless in-wheel motor circuit configuration

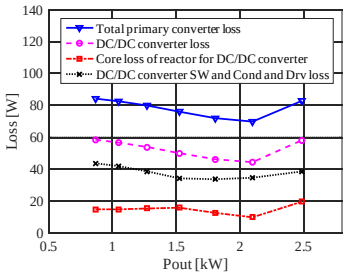

Fig. 8. Primary converter loss break down of chopper mode

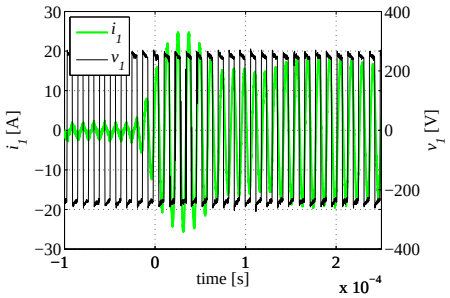

(a) primary current and voltage

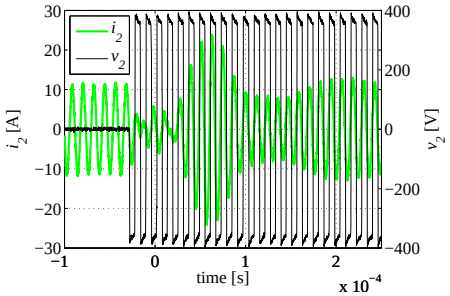

(b) secondary current and voltage

Fig. 9. Intermittent synchronous rectification control

Switching losses are evaluated as follows.

$$P_{sw,HB}\left(P, V_{batt}, V_2\right) = 2f_0\left(E_{on}\left(I_{1,1}, V_{batt}\right) + E_{off}\left(I_{1,1}, V_{batt}\right)\right) \quad (5)$$

Fig. 6 shows the results of the efficiency comparison between chopper mode system and the phase shift system. In addition, Fig. 7 shows experimental values of primary converter loss comparison of the chopper mode system and the phase shift mode system (primary DC/DC converter is bypassed).

To verify the loss model, the measured values are acquired in actual W-IWM. Here, if the secondary coil terminals are short-circuited, the switching mode of secondary converter is called short mode. If all the secondary converter switches are OFF, the switching mode is called rectification mode. In all the operating point, the WIWM has been used in such a way that $V_1 = V_2$.

It means that the receiving-side converter does not operate in short mode, and consequently all the transmitting-side inverter controls are compared in rectification mode. Although loss model of the phase shift indicates a very satisfactory performance, some errors in the case of the chopper mode system are observed. This error is mainly due to inaccurate modeling of the inductor loss. As expected from the comparison between chopper and the phase shift method, it appears that the phase-shift scheme is more efficient if V_1 is at the maximum and the H-bridge converter is operated in quasi square-wave mode. In this case the phase shift method is close to the chopper system, because the switching losses of the H-bridge converter are reduced and there is no loss in the previous DC/DC converter. Consequently the efficiency is improved.

However, since the chopper is expected to be used during most of the travel pattern of a normal W-IWM, chopper system during normal driving is considered as appropriate.

Fig.8 shows the loss break down of transmitter side converter of chopper mode system. As mentioned above, total loss of the converter is measured by experiments. The DC/DC converter losses are composed by core loss of inductor of the DC/DC converter, switching loss of IGBT of the DC/DC converter, conduction loss of the IGBT and gate driving loss of the IGBT. The loss of the H-bridge converter can be calculated by (5) and other formula of conduction loss estimation. The switching loss, conduction loss and gate driving loss of the DC/DC converter can be calculated. Therefore, the authors can estimate the core loss of the inductor of the DC/DC converter by subtracting the H-bridge converter loss and the IGBT loss from total converter loss.

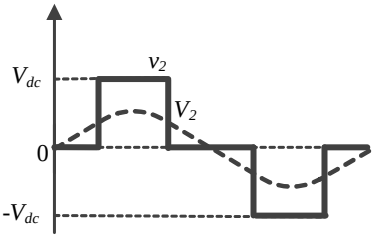

(a) secondary phase shift control

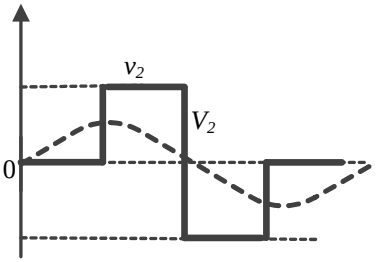

(b) secondary symmetric synchronous rectification control

Fig. 10. 2 type of synchronous rectification control

IV. High efficiency of the W-IWM system in the secondary side

In this section, we discuss the comparison among the phase shift control, intermittent synchronous rectification control and symmetric rectification control in the receiving side. Fig.9 shows experimental results of intermittent synchronous rectification control[14]. Fig.10 shows the concept of two type of synchronous rectification control as above.

The H-bridge circuit on the wheel side is switched between a short-circuit state (v_2 = 0) and the diode rectification state to match the V_{dc} programmed within the hysteresis band. The period of this switching is at a much lower frequency than the resonant frequency f_0. Conduction losses in the rectifier mode can be reduced by implementing synchronous rectification techniques to avoid conduction of the antiparallel diode of SiC[15]. When evaluating the system efficiency, the effect of the two-mode control must be taken into account. Power transmission current i_1 of the receiving-side converter circuit is almost zero during short mode. In rectification mode, receiving current i_2 is considered to be constant, as the short transient phenomenon, after mode transition is neglected. Here, the maximum value of the transmission current $I_{1,max}$ is

$$I_{1,max} = \frac{V_2}{2\pi f_0 L_m} = \frac{\sqrt{2}V_{dc}}{\pi^2 f_0 L_m}. \tag{6}$$

The receiving-side converter duty is related to the power P and the transmitting side voltage V_1. Here D_2 is the ratio between V_2 maximum value and the V_2 fundamental wave rms value :

$$D_2 = \frac{V_2}{\frac{2\sqrt{2}}{\pi \cdot V_{dc}}}. \tag{7}$$

By combining (2) and (7), the following equation is derived:

$$V_2 = D_2 \frac{2\sqrt{2}}{\pi} V_{dc} = \frac{P}{V_1} 2\pi f_0 L_m \tag{8}$$

Then, in same way for (8) and (7), the duty becomes:

$$D_2 = \frac{P}{V_1 V_{dc}} \frac{\pi^2 f_0 L_m}{\sqrt{2}} \leq 1. \tag{9}$$

Assuming a much lower switching frequency than f_0, the rms value of the transmission current with intermittent synchronous rectification $I_{1,rms,2M}$ is as follows.

$$\begin{aligned} I_{1,rms,2M} &= \sqrt{\frac{1}{T}\int_0^{D_2 T} i_1(t) \cdot dt} \\ &= I_{1,max} \cdot \sqrt{D_2} \\ &= \frac{I_{1,rms,phsh}}{\sqrt{D_2}}. \end{aligned} \tag{10}$$

where $I_{1,rms,phsh}$ is the rms value of the transmission current due to the phase shift control of the receiving converter. In (10), $D_2 < 1$. Therefore, increasing in the transmitting-side current rms value is realized with respect to the phase shift control.

Here the power P needed for wireless power transmission is constant, showing various efficiency calculation results when the power of the only cover the P has a transmission voltage V_{send} a variable that can be power transmission.

V. Loss and efficiency calculation in secondary side

Fig.11 shows efficiency calculation results intermittently synchronize the receiving side to the power transmission side to the chopper system rectification system (2mode with SR), the phase shift method, each with symmetric synchronous rectification at V_{dc} = 350 [V].

Fig.12 shows loss break down of three methods above mentioned. This calculation has been done at P = 500 [W].

According (10), there is optimal point of efficiency of the system by operating V_{send}. Fig.11 shows optimal operating point of high efficiency. This figure shows we can truck the point of optimal efficiency by operating V_{send} depending on the required P.

The method with the best efficiency of the three is intermittent synchronous rectification control to perform a zero-voltage zero-current switching. The efficiency of symmetric synchronous rectification to perform the part zero voltage zero current switching is also acceptable.

However, intermittent synchronous rectification control for short-circuiting radiates electromagnetic noise larger transient current flows during a short-circuit of the power receiving resonator.

VI. Conclusion

This paper proposes two methods of DC/DC chopper control and phase shift control for transmitting side, aiming to high efficiency. The DC/DC chopper method is better

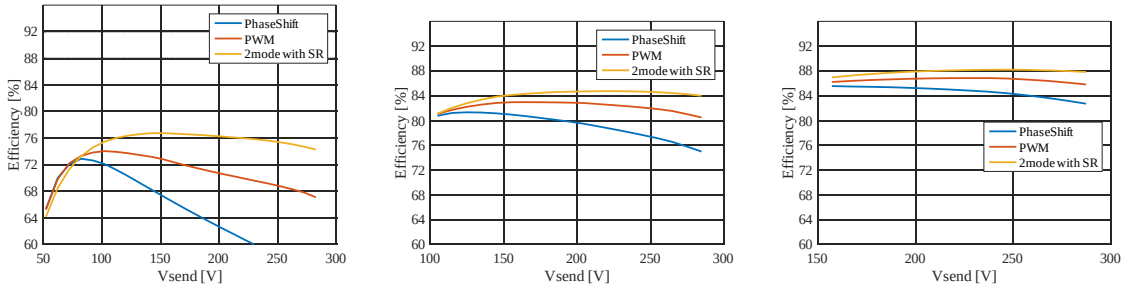

(a) P=500 W (b) P=1000 W (c) P=1500 W

Fig. 11. Calculation results by using DC/DC chopper control on transmitter side

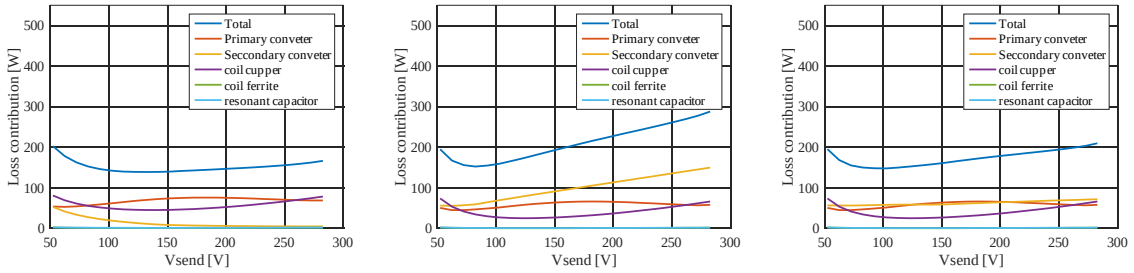

(a) The power-receiving-side: intermittent synchronous rectification control (b) The power-receiving-side: phase shift control control (c) The power-receiving-side: symmetric synchronous rectification control

Fig. 12. Loss break down results on secondary side (P = 500 W, transmitting side: DC/DC chopper control)

than phase shift control. In addition, intermittent synchronous rectification control, symmetric synchronous rectification control and phase shift control are analyzed. Among the three proposed methods, symmetric synchronous rectification control is optimized considering the balance performance of the harmonic and the losses for W-IWM.

ACKNOWLEDGMENT

The research presented in this paper was funded in part by the Ministry of Education, Culture, Sports, Science and Technology grant (No. 26249061). The authors would like to express their deepest appreciation to the Murata Manufacturing Co., Ltd. for providing the laminated ceramic capacitors (U2J characteristics) used in these experiments.

REFERENCES

[1] Y. Hori: “Future Vehicle Driven by Electricity and Control Research on Four Wheel Motored “UOT Electric March II””, IEEE Trans. IE, Vol. 51, No. 5, pp. 954–962 (2004)

[2] S. Harada, H. Fujimoto: “Range extension control system for electric vehicles during acceleration and deceleration based on front and rear driving-braking force distribution considering slip ratio and motor loss”, 39th Annual Conference of the IEEE Industrial Electronics Society (IECON), pp. 6626–6631 (2013)

[3] S. Murata: “Vehicle Dynamics Innovation with In-Wheel Motor,” Proc. JSAE EVTeC’11, 20117204, Yokohama, (2011).

[4] Naoya Ochi, Hiroshi Fujimoto and Yoichi Hori: “Proposal of Roll Angle Control Method Using Positive and Negative Anti-dive Force for Electric Vehicle with Four In-wheel Motors”, IEEE International Conference on Mechatronics, Vicenza, Italy, pp.815–820, (2013)

[5] Toyota Motor Corporation, P2012–223041A 2012. (in Japanese)

[6] A. Kurs, A. Karalis, R. Moffatt, J. D. Joannopoulos, P. Fishe, and M. Soljacic: “Wireless Power Transfer via Strongly Coupled Magnetic Resonances”, in Science Express on 7 June 2007, Vol. 317, No. 5834, pp. 83–86 (2007)

[7] T. Imura, H. Okabe, T. Uchida, and Y. Hori: “Flexibility of Contactless Power Transfer using Magnetic Resonance Coupling to Air Gap and Misalignment for EV”, IEEE Electric Vehicle driven on Electric Vehicle Symposium 24, (2009).

[8] M. Kato, T. Imura, and Y. Hori: “The Characteritics when Changing Transmission Distance and Load Value in Wireless PowerTransfer via Magnetic Resonance Coupling”, IEEE Telecommunications Energy Conference INTELEC (2012)

[9] D. Gunji, T. Imura, H. Fujimoto, ”Fundamental Research on Control Method for Power Conversion Circuit of Wireless In-Wheel Motor using Magnetic Resonance Coupling”, IEEJ Transaction on Industry Applications, Vol. 135, No. 3 pp.182–191 (2015)

[10] M. Sato, G. Yamamoto, D. Gunji, T. Imura. and H. Fujimoto, “Development of Wireless In-Wheel Motor using Magnetic Resonance Coupling,” Transactions on Power Electronics , IEEE 2015 9, Vol. 31, No. 7

[11] H. Fujimoto, T. Miyajima, and J. Amada: “Development of Electric Vehicle with Variable Drive Unit System”, International Electric Vehicle Technology Conference & Automotive Power Electronics Japan 2014 (2014)

[12] SAE International: “Wireless charging advances with selection of 85-kHz charging frequency”, http://articles.sae.org/12647/(2013)

[13] G. Guidi, “Minimization of Converter Ratings for MW-scale Inductive Charger Operated under Widely Variable Coupling Conditions,” Wireless Power (WoW), 2015 IEEE PELS Workshop on, (2015).

[14] M. Sato, G. Guidi, T. Imura, H. Fujimoto: Experimental Verification for Wireless In-Wheel Motor using Synchronous Rectification with Magnetic Resonance Coupling, International Electric Vehicle Technology Conference & Automotive Power Electronics Japan (2016), 2016/5/25-2016/5/27, Yokohama, Japan.

[15] ROHM Co., Ltd. : “bsm120d12p2c005 datasheet”, http://rohmfs.rohm.com/en/products/databook/datasheet/discrete/sic/power_module/bsm120d12p2c005.pdf